福井大学リポジトリ
UNIVERSITY OF FUKUI
REPOSITORY

Timing-performance evaluation of Cherenkov-based radiation detectors

メタデータ	言語: eng 出版者: 公開日: 2020-07-15 キーワード (Ja): キーワード (En): 作成者: Ota, R, Nakajima, K, Hasegawa, T, Ogawa, I, Tamagawa, Y メールアドレス: 所属:
URL	http://hdl.handle.net/10098/10954

copyright 2019 Elsevier B.V. All rights reserved

Nuclear Inst. and Methods in Physics Research, A 923 (2019) 1–4

Contents lists available at ScienceDirect

Nuclear Inst. and Methods in Physics Research, A

journal homepage: www.elsevier.com/locate/nima

Timing-performance evaluation of Cherenkov-based radiation detectors

R. Ota [a,b,1,*], K. Nakajima [b], T. Hasegawa [c], I. Ogawa [b], Y. Tamagawa [b]

[a] Central Research Laboratory, Hamamatsu Photonics K. K., Hamamatsu, Japan
[b] Faculty of Engineering, University of Fukui, Fukui, Japan
[c] School of Allied Health Sciences, Kitasato University, Sagamihara, Japan

ARTICLE INFO

Keywords:
Cherenkov radiation
Lead fluoride
Microchannel plate photomultiplier tube
Coincidence time resolution

ABSTRACT

With the upgradation of detector components, such as scintillators and photodetectors, the PET-image signal-to-noise ratio of time-of-flight positron emission tomography (TOF-PET) systems has been improved, compared to those of ordinary nonTOF-PET systems. A TOF-PET with an ultrahigh time resolution, for example a coincidence time resolution (CTR) better than few tens of picoseconds, can not only improve the image quality, but also remove the image reconstruction process, significantly impacting medical imaging. Therefore, it is crucial to develop a high-time resolution PET detector. We focus on the prompt emission of Cherenkov radiation, owing to the instantaneousness of which, a high time resolution can be expected. One of the candidates for the Cherenkov radiator is lead fluoride (PbF_2) due it has excellent properties, including transparency toward the ultraviolet region, high refractive index (n = 1.82), and high density (7.77 g/cm^3). Moreover, it does not contain radioisotopes, unlike lutetium-based scintillators, which are commonly used in the currently available TOF-PET detectors. In this work, we experimentally investigate the timing performance of PbF_2-based Cherenkov detectors, breaking down the timing performance into physical components. 3×3×5 mm^3 and 9.6×9.6×5 mm^3 PbF_2 crystals are used as Cherenkov radiators; both are attached to a microchannel plate photomultiplier tube (MCP-PMT) because the single channel MCP-PMT is one of the best photodetectors in terms of the SPTR, which is 25 ps full width at half maximum (FWHM). All the surfaces, except the end surface where the MCP-PMT is connected, are wrapped in black tape to suppress the reflections of the Cherenkov photons in the crystal. The CTR is measured by placing a detector pair face-to-face, using an^{22}Na point source, and an oscilloscope at 20 GS/s with a set bandwidth of 4.2 GHz. A CTR of 46.9 ps FWHM, corresponding to a position resolution of 7.0 mm, is obtained, consistent with our simulation results.

1. Introduction

There is a requirement for radiation detectors with high timing performances in time-of-flight positron emission tomography (TOF-PET) applications. The advancements in detector timing resolution have improved the image quality of PET systems, in terms of the signal-to-noise ratio (SNR). The contribution of the timing resolution is described by the following equation:

$$\mathrm{SNR}_{\mathrm{TOF\text{-}PET}}/\mathrm{SNR}_{\mathrm{nonTOF\text{-}PET}} = \sqrt{2D/(c\Delta T)}, \quad (1)$$

where D is the effective diameter of an object, c is the speed of light, and ΔT is the coincidence time resolution (CTR) of a PET detector [1]. If a CTR of 30 ps full width at half maximum (FWHM) is achieved, the position resolution along the line of response (LOR) is equivalent to 4.5 mm FWHM. As this position resolution is of the same order of the spatial (x, y) resolution of recent clinical TOF-PET systems [2], the direct determination of the annihilation point along the LOR, in clinical TOF-PET systems, is achievable [3]. Direct localization enables the removal of artifacts caused by image reconstruction processes, significantly impacting medical imaging. Therefore, it is crucial to pursue ultrahigh timing resolution down to 30 ps FWHM.

The timing resolution of scintillation-based detectors has been studied theoretically and experimentally for several decades [4–6]. Various research groups have already obtained CTRs better than 100 ps FWHM, using scintillation-based radiation detectors [7,8]. These research has established that prompt emissions, which occur before the scintillation luminescence, play an important role in improving the timing resolution [9–11]. One of the prompt emissions that can be detected by photodetectors, such as photomultiplier tubes (PMTs) and silicon photomultipliers (SiPMs), is the Cherenkov radiation. In addition to prompt emission, single photon timing resolution (SPTR) also plays an important role [3,12].

The timing performance of a Cherenkov-based detector for PET has been reported, using a fast photodetector [13]. The CTRs of a pair of detectors, composed of a lead fluoride (PbF_2) crystal and a multianode microchannel plate PMT (MA-MCP-PMT, Hamamatsu Photonics K. K.),

* Corresponding author at: Central Research Laboratory, Hamamatsu Photonics K. K., Hamamatsu, Japan.
E-mail address: ryosuke.ota@crl.hpk.co.jp (R. Ota).
[1] Postal address: 5000, Hirakuchi, Hamakita-ku, Hamamatsu 434-8601, Japan.

https://doi.org/10.1016/j.nima.2019.01.034
Received 18 June 2018; Received in revised form 9 November 2018; Accepted 12 January 2019
Available online 22 January 2019
0168-9002/© 2019 Elsevier B.V. All rights reserved.

with an SPTR of $\sigma = 27$ ps, were 71 and 95 ps FWHM using 5- and 15-mm thick radiators, respectively [13]. These results correspond to the simulation results of ref. [12], according to which, the CTR can be improved, if the SPTR is better than that of the MA-MCP-PMT. However, it has not been experimentally proved that a better SPTR definitely provides a better CTR.

In this paper, we present the experimentally obtained CTRs, using detectors composed of a PbF_2 crystal and single channel MCP-PMT. A single channel MCP-PMT is used because it is one of the photodetectors with an SPTR better than that of the MA-MCP-PMT. The potential capability of a single-channel MCP-PMT as a fast timing detector is demonstrated.

2. Materials and methods

2.1. Detector

The MCP-PMT (R3809, Hamamatsu Photonics K. K.) was used as the photodetector because it has the highest timing performance against a single photon; the SPTR is 25 ps FWHM [14], which is better by more than twice, compared to that of the MA-MCP-PMT used in ref. [13].

The number of emissions of Cherenkov photons within the Cherenkov photon wavelength interval between λ_1 and λ_2 ($\lambda_1 < \lambda_2$) is theoretically described by the following equation:

$$N = 2\pi\alpha L\left(\frac{1}{\lambda_1} - \frac{1}{\lambda_2}\right)\left(1 - \left(\frac{1}{n\beta}\right)^2\right), \quad (2)$$

where N is the number of emitted Cherenkov photons, α is the fine structure constant, L is the path length of a charged particle through a dielectric medium, n is the refractive index of the dielectric medium, and β is the speed of the charged particle. Therefore, a small λ_1 and large n are required for increasing N. Thus, for a Cherenkov radiator, transparency toward the ultraviolet (UV) region and a high refractive index are required for detecting numerous Cherenkov photons. Here, a PbF_2 crystal is employed as the Cherenkov radiator because of its excellent properties, namely, high transparency and refractive index [15]. Two types of PbF_2 crystals are used in this work, $3 \times 3 \times 5$ mm^3 and $9.6 \times 9.6 \times 5$ mm^3, for investigating the components of the timing performance. The MCP-PMT and $3 \times 3 \times 5$ mm^3 PbF_2 crystal were glued using optical grease (KE-420, Shin-Etsu Chemical), as shown in Fig. 1-(a), whereas the $9.6 \times 9.6 \times 5$ mm^3 PbF_2 crystal was only placed on the housing surface of the MCP-PMT, as shown in Fig. 1-(b). All the crystal surfaces, except the detector-side surface, were wrapped in black tape (Super 33+, 3M) to suppress the reflections of the Cherenkov photons in the radiator.

2.2. Experimental setup

Fig. 2 depicts the experimental setup for evaluating the CTR. Each detector pair shown in Fig. 1-(a) was placed face-to-face. An ^{22}Na point source, collimated using a 0.5-mm slit, was located between the detectors. A high voltage of −3100 V was applied to both MCP-PMTs. The signals were monitored by an oscilloscope (DSO-404A, Keysight) at 20 GS/s with a set bandwidth of 4.2 GHz.

Figs. 3-(a), -(b), -(c), and -(d) show the experimental setups for investigating the interaction points of the γ-rays. Because the MCP contains lead glass, the MCP itself is sensitive to γ-rays. Moreover, as the MCP channel diameter is only 6 μm, it is easy for energetic photoelectrons to escape to the channel surface. Finally, the photoelectrons are multiplied along the MCP channel. In the case of Fig. 3-(a), nine types of coincidence combinations are possible, as shown in Table 1. Hence, it is expected that the distribution of the time difference between the two detectors consists of nine components. On the other hand, in the case of Fig. 3-(b), -(c), and -(d), only one type of coincidence combination for unscattered γ-rays is permitted, i.e., PbF_2-PbF_2, window-face-plate (WFP)-WFP, and WFP-MCP, respectively. Therefore, it is expected that the distribution will contain only one component. From the above-mentioned figures, the distribution obtained from the experiment depicted in Fig. 3-(a) can be broken down into each coincidence combination.

Table 1
Coincidence combinations of a pair of detectors.

		Detector-1		
		PbF_2	WFP	MCP
Detector-2	PbF_2	Comb. 1	Comb. 2	Comb. 3
	WFP	Comb. 4	Comb. 5	Comb. 6
	MCP	Comb. 7	Comb. 8	Comb. 9

The spline curves of the analog signals from the two detectors were obtained event-by-event, using the TSpline3 class method in ROOT, which is an object-oriented data analysis framework [16]; the pulse heights of the signals were numerically calculated using the spline curves. As the timing pick-off threshold level, a pulse height with a level of 10% was employed to avoid time walk correction. As the ratio of the number of signals, which overflowed the oscilloscope's range, to total number of signals was less than 5%, the overflow signals were not analyzed in this work.

3. Results and discussion

Fig. 4-(a) illustrates the time difference between the signals from the two detectors, obtained using the experimental setup shown in Fig. 2. The broken line depicts the fitting result; the CTR is 46.9 ps FWHM, which corresponds to a position resolution of 7.0 mm. Thus, a position resolution better than 10 mm was achieved using the existing detectors. The two small peaks around the center peak were caused by the direct interaction of an annihilation γ-ray with the MCP. This ultrahigh timing performance is due to the prompt emission of Cherenkov photons and the good SPTR of the MCP-PMTs. According to ref. [12], for a PbF_2 thickness of 5 mm and SPTR of $\sigma = 10$ ps, the expected CTR is approximately 34 ps. The difference between the simulation and experimental result may be due to electrical noise, and the difference in the radiator dimensions. Fig. 4-(b) shows pulse height distributions, each of which is for different types of interactions within a time window described in Fig. 4-(a).

Fig. 5 depicts the time difference histograms between the two detectors, obtained using the experimental setups shown in Fig. 3-(a), -(b), -(c), and -(d), respectively. In setup (a) as well as in Fig. 4, three peaks are clearly visible. The interval between each peak is approximately 240 ps. On the other hand, in setup (b) and (c), only one peak can be seen because only one coincidence combination is permitted. In setup (d), although three peaks are visible, the right-side peak shows the highest intensity. The photoelectrons induced in the MCP are promptly multiplied; however, those generated in the cathode plane need to drift to the MCP. The supplied voltage, and distance between the cathode plane and MCP is approximately 900 V and 2.0 mm, respectively. Using this information, the drift time can be estimated to be 225 ps, if a simple constant acceleration motion is assumed against the photoelectrons. This value nearly corresponds to the experimental result of 240 ps, shown in Fig. 5. Finally, we determined that the MCP-PMT itself is sensitive to 511-keV γ-rays. This worsens the position resolution because the γ-ray interaction position, namely, the Cherenkov radiator or MCP, cannot be distinguished. Therefore, the lead glass should be removed from the MCP to render the MCP itself insensitive to γ-rays.

4. Conclusion

In this work, excellent timing performance was obtained using a Cherenkov-based detector, owing to its prompt emission and good SPTR. It was established that a CTR of 46.9 ps, corresponding to a position resolution of 7.0 mm, for annihilation γ-rays, is possible using the existing detectors. Thus, further improvement of the photodetector, in terms of the SPTR in particular, can definitely improve the timing performance and render the reconstruction process in TOF-PET systems unnecessary.

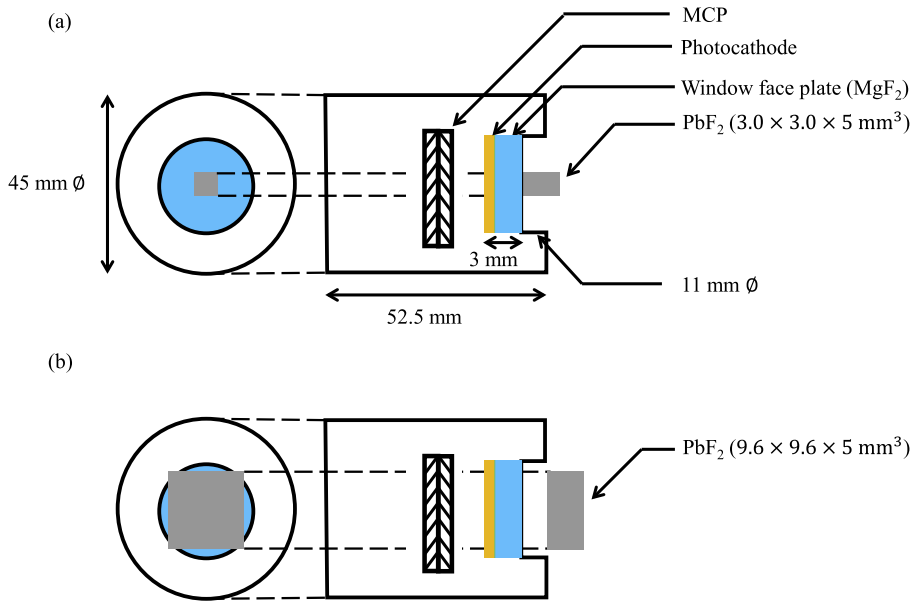

Fig. 1. Sectional views of the detectors evaluated in this paper. The PbF_2 crystals were wrapped in black tape, except for the detector-side surface. (a) The $3 \times 3 \times 5$ mm^3 PbF_2 crystal was attached to the MCP-PMT using optical grease, and (b) the $9.6 \times 9.6 \times 5$ mm^3 PbF_2 crystal was placed on the housing surface of the MCP-PMT.

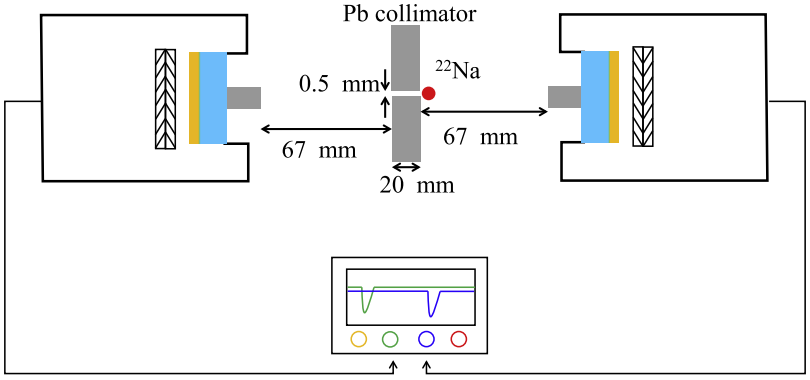

Fig. 2. Experimental setup for CTR evaluation. Two $3 \times 3 \times 5$ mm^3 PbF_2 crystals were placed face-to-face. An ^{22}Na point source was used as the β^+ emitter. A DSO-404A oscilloscope was activated at 20 GS/s with a set bandwidth 4.2 GHz.

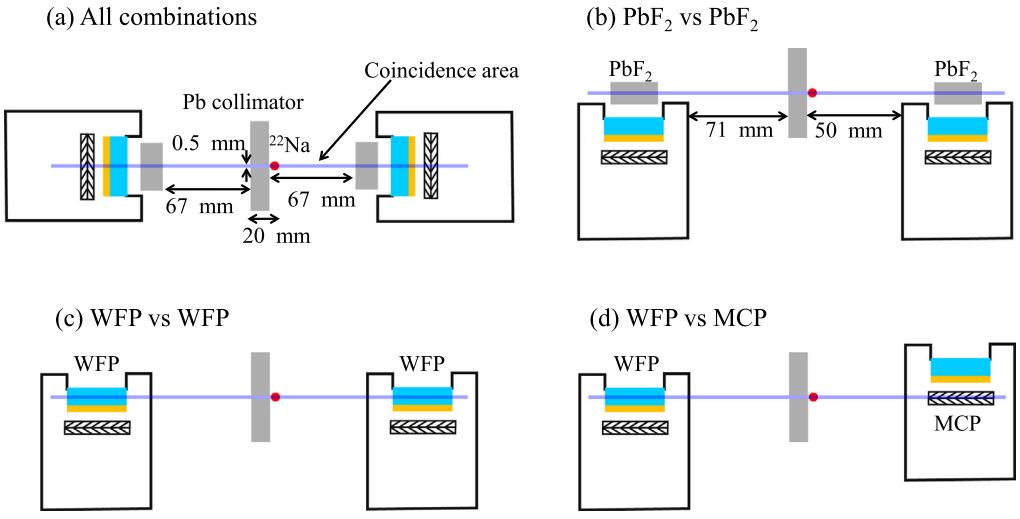

Fig. 3. Experimental setups for investigating the γ-ray interaction point. (a) A pair of detectors was located face-to-face, (b) a pair of PbF_2 crystals, (c) two WFPs of the MCP-PMT, and (d) a WFP and MCP, were located side-by-side, respectively.

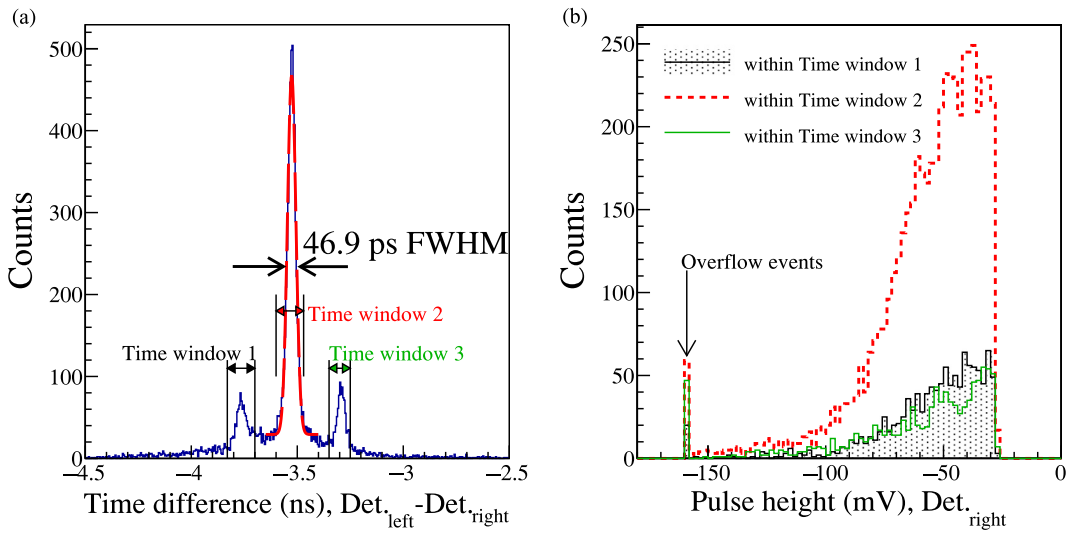

Fig. 4. (a) Distribution of the time difference between the signals from the two detectors using two $3\times3\times5$ mm^3 PbF_2 crystals coupled with the MCP-PMTs. The broken line indicates the fitting result of "a single Gaussian + constant". The center peak shows that the CTR is 46.9 ps FWHM. The two small peaks around the center peak are caused by the direct interaction of an annihilation γ-ray with the MCP and (b) Pulse height spectra of the right-side detector, within each time window described in Fig. 5-(a).

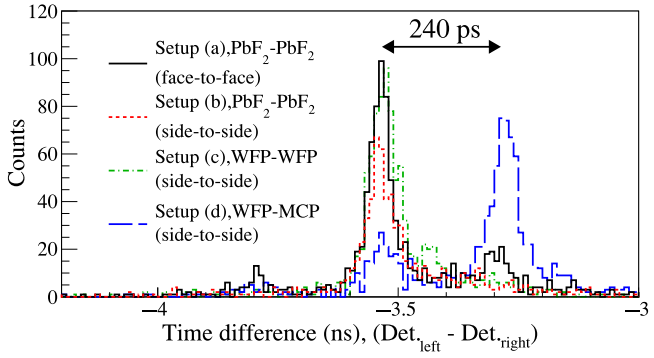

Fig. 5. Time-difference histograms, obtained from several experimental setups. For setup (a) and (b), $9.6\times9.6\times5$-mm^3 PbF_2 crystals were placed on the MCP-PMTs. It was determined that the peak position depends on the interaction position of the γ-rays. This can be explained by the finite drift time of the electron from the photocathode to the MCP.

Acknowledgments

The authors thank Tomohide Omura and Ryoko Yamada of the Central Research Laboratory of Hamamatsu Photonics for their assistance and significant discussions.

References

[1] M. Conti, State of the art and challenges of time-of-flight PET, Phys. Med. 25 (2009) 1–11.
[2] S. Vandenberghe, et al., Recent developments in time-of-flight PET, EJNMMI Phys. 3 (2016).
[3] S. Gundacker, et al., Measurement of intrinsic rise times for various L(Y)SO and LuAG scintillators with a general study of prompt photons to achieve 10 ps in TOF-PET, Phys. Med. Biol. 61 (2016) 2802–2837.
[4] R.F. Post, L.I. Schiff, Statistical limitations on the resolving time of a scintillation counter, Phys. Rev. 80 (1950) 1113.
[5] S. Seifert, et al., A comprehensive model to predict the timing resolution of SiPM-based scintillation detectors: theory and experimental validation, Trans. Nucl. Sci. 59 (2012) 190–204.
[6] S. Seifert, et al., The lower bound on the timing resolution of scintillation detectors, Phys. Med. Biol. 57 (2012) 1797–1814.
[7] J.W. Cates, C.S. Levin, Advances in coincidence time resolution for PET, Phys. Med. Biol. 61 (2016) 2255–2264.
[8] S. Gundacker, et al., State of the art timing in TOF-PET detectors with LuAg, GAGG and L(Y)SO scintillators of various sizes coupled to FBK-SiPMs, J. Instrum. 11 (2016) P08008.
[9] M. Miyata, et al., Development of TOF-PET using Cherenkov radiation, J. Nucl. Sci. Tech. 43 (2006) 339–343.
[10] P. Lecoq, et al., Factors influencing time resolution of scintillators and ways to improve them, Trans. Nucl. Sci. 57 (2010) 2411–2416.
[11] P. Lecoq, et al., Can transit phenomena help improving time resolution in scintillations? Trans. Nucl. Sci. 61 (2014) 229–234.
[12] R. Ota, et al., Cherenkov radiation-based three-dimensional position-sensitive PET detector: A Monte Carlo study, Med. Phys. 45 (2018) 1999–2008.
[13] S. Korpar, et al., Study of TOF-PET using Cherenkov light, Nucl. Instrum. Methods A 654 (2011) 532–538.
[14] http://www.hamamatsu.com, Data sheet for R3809U-50 series, accessed 26th Feb. 2018.
[15] D.F. Anderson, et al., LEAD FLUORIDE: An ultra-compact Cherenkov radiator for EM calorimetry, Nucl. Instrum. Methods A 290 (1990) 385–389.
[16] R. Brun, F. Rademakers, ROOT-An object-oriented data analysis framework, Nucl. Instrum. Methods A 389 (1997) 81–86.